

Minimizing Misclassification of Damage using Extreme Value Statistics

Hoon Sohn¹, Hyun Woo Park², Kincho H. Law³, and Charles R. Farrar⁴

¹ *Department of Civil and Environmental Engineering
Carnegie Mellon University, Pittsburgh, PA15213, USA*

² *Korea Earthquake Engineering Research Center
Seoul National University, Seoul 151-742, Korea*

³ *Department of Civil and Environmental Engineering
Stanford University, CA 94305, USA*

⁴ *Engineering Sciences and Application Division
Los Alamos National Laboratory, NM 87545, USA*

hsohn@andrew.cmu.edu, hwpark91@snu.ac.kr, law@stanford.edu, farrar@lanl.gov

ABSTRACT

Structural health monitoring is a process of evaluating and ensuring the safety and integrity of structural systems by converting sensor data into structural health monitoring information. The first and most important objective of structural health monitoring is to ascertain with confidence if damage is present or not. The idea is to characterize only the normal condition of a structure and the baseline data are used as a reference. When data are measured during continuous monitoring, the new data are compared with the reference. A significant deviation from the reference will signal damage. This decision-making procedure necessitates the establishment of a decision boundary. Choosing the decision boundary is often based on the assumption that the distribution of the data is Gaussian in nature. While the problem of damage detection focuses attention on the outliers or extreme values of the data, i.e. those points in the tails of the distribution, the establishment of the decision boundary based on the normality assumption weighs the central population of the data. This unwarranted assumption about the nature of the data distribution can significantly impair the performance of a structural health monitoring system by increasing false positive and negative indications of damage. In this study, a robust and automated damage classifier is developed by properly modeling the tails of the distribution using extreme value statistics.

¹ Assistant Professor

² Research Associate

³ Professor

⁴ Technical Staff Member

1. INTRODUCTION

The first and most important objective of any damage identification algorithm is to ascertain with confidence if damage is present. Considering most real world applications of damage detection, this detection must be accomplished in an unsupervised learning mode. Here, the term 'unsupervised learning' indicates that data from a damaged state are not used to aid in the damage detection process. The objective of the unsupervised damage detection is to establish a statistical model of the features extracted from the normal condition of structures and thereafter to signal significant departures from this normal condition.

The statistical modeling of the features extracted from the measured data can be accomplished in several ways. The most direct methods seek to model the probability distribution of the normal condition using *a priori* training data. For instance, the outlier approach (Worden *et al.* 2000a) often assumes the damage sensitive features have a Gaussian distribution and the model parameters such as the mean vector and the covariance matrix are estimated from the data. More sophisticated approaches use Gaussian mixture models (Roberts 1998, 2000) or kernel density estimates (Worden *et al.* 2000b). The main limitation of all of these methods is that they make an unwarranted assumption about the nature of the feature distribution. For instance, the statistical modeling based on these methods weigh on central statistics such as the mean vector and the covariance matrix, and the analysis is largely insensitive to the tails of the distribution. However, damage detection is mainly concerned with the data points near the tails of the distribution. This unwarranted assumption about the nature of the feature distribution can lead to false positive and false negative indications of damage.

The major problem with modeling the undamaged condition of a system is that the functional form of the distribution is unknown and there are an infinite number of candidate distributions that may be appropriate for the prediction applications. Furthermore, in some cases, only extreme values of events may be recorded due to sensor or storage limitations. Therefore, modeling the data as a parent distribution could also bring about erroneous results. For example, seismic stations are primarily interested in recording strong ground motions, which have magnitudes beyond certain strength to affect people and their environment (Kramer 1996). Currently, a choice among the infinite distributions is made by knowledgeable operator and then the parameter estimation is based on training data. This process is largely subjective. Any choice of distribution and parameters will also constrain the behavior of the tails to that prescribed distribution.

In fact, there is a large body of statistical theory that is explicitly concerned with modeling the tails of distributions, and these statistical procedures can be applied to the problem of damage detection. The relevant field is referred to as extreme value statistics (EVS), a branch of order statistics. EVS has been widely used in engineering problems in fields like meteorology, hydrology, ocean engineering, pollution studies, strength of materials and so on. This paper illustrates that EVS can be used to minimize misclassification of damage for structural health monitoring applications and a procedure to automatically estimate the parameters of the extreme value distributions is presented.

The layout of this paper is as follows: Section 2.1 introduces three types of extreme value distributions consisting of Gumbel, Weibull, and Frechet distributions. Section 2.2 describes the parameter estimation of extreme value distributions. Section 2.3 provides a brief description of constrained nonlinear optimization technique for estimating the extreme distribution parameters. Section 3.1 shows a comparison between thresholds of the damage index calculated using Gaussian assumption with those calculated using EVS for numerical data generated from different probability density functions. Section 3.2 demonstrates validity of the parameter estimation method using real sample data and comparison studies with other methods are provided. Section 3.3 explores the integration of EVS into delamination detection in a composite plate using the time reversed Lamb waves. Conclusions and further recommendations are provided in Section 4.

2. Extreme Value Statistics and Parameter Estimation of Extreme Value Distributions

2.1 Extreme Value Statistics

The Gaussian distribution occupies its central place in statistics for a number of reasons; not least

is the central limit theorem (Benjamin and Cornell, 1970). The central limit theorem states that if $\{X_1, X_2, \dots, X_n\}$ is a set of random variables with arbitrary distributions, the sum variable $X_\Sigma = X_1 + X_2 + \dots + X_n$ will have a Gaussian distribution as $n \rightarrow \infty$. Although this theory is arguably the most important limiting theorem in statistics, it is not the only one. If the problem at hand is concerned with the tails of distributions, there is another theorem that is more appropriate.

Suppose that one is given a vector of samples $\{X_1, X_2, \dots, X_n\}$ from an arbitrary *parent distribution*. The most relevant statistic for studying the tails of the parent distribution is the maximum operator, $\max(\{X_1, X_2, \dots, X_n\})$, which selects the point of maximum value from the sample vector. Note that this statistic is relevant for the right tail of a univariate distribution only. For the left tail, the minimum should be used. The pivotal theorem of EVS states that in the limit as the number of vector samples tends to infinity, the induced distribution on the maxima of the samples can only take one of three forms: Gumbel, Weibull, or Frechet (Fisher and Tippett, 1928).

$$\text{FRECHET: } \bar{F}(x) = \begin{cases} \exp\left[-\left(\frac{\delta}{x-\lambda}\right)^\beta\right] & \text{if } x \geq \lambda \\ 0 & \text{otherwise} \end{cases} \quad (1)$$

$$\text{WEIBULL: } \bar{F}(x) = \begin{cases} 1 & \text{if } x \geq \lambda \\ \exp\left[-\left(\frac{\lambda-x}{\delta}\right)^\beta\right] & \text{otherwise} \end{cases} \quad (2)$$

$$\text{GUMBEL: } \bar{F}(x) = \exp\left[-\exp\left(-\frac{x-\lambda}{\delta}\right)\right] \quad -\infty < x < \infty \text{ and } \delta > 0 \quad (3)$$

In a similar fashion, there are only three types of distribution for the minima of the samples;

$$\text{FRECHET: } \underline{F}(x) = \begin{cases} 1 - \exp\left[-\left(\frac{\delta}{\lambda-x}\right)^\beta\right] & \text{if } x \leq \lambda \\ 1 & \text{otherwise} \end{cases} \quad (4)$$

$$\text{WEIBULL: } \underline{F}(x) = \begin{cases} 0 & x \leq \lambda \\ 1 - \exp\left[-\left(\frac{x-\lambda}{\delta}\right)^\beta\right] & x > \lambda \end{cases} \quad (5)$$

$$\text{GUMBEL: } \underline{F}(x) = 1 - \exp\left[-\exp\left(\frac{x-\lambda}{\delta}\right)\right] \quad -\infty < x < \infty \text{ and } \delta > 0 \quad (6)$$

where λ , α , and β are the model parameters, which should be estimated from the data.

When samples of maximum or minimum data from a number of n -point populations are given, it is possible to select an appropriate limit distribution and fit a parametric model to the data. It is also possible to fit a model to portions of the parent distribution's tails, as the distribution of the tails is equivalent to the appropriate extreme value distribution. Once the parametric model is obtained, it can be used to compute an effective threshold for novelty based on the true statistics of the data as opposed to statistics based on an unwarranted assumption of a Gaussian distribution.

2.2 Parameter Estimation of Extreme Value Distributions

A least squares method using the generalized weighted least squares is employed to find the best-fit extreme value distribution.

$$\text{Min}_{\theta} \pi = \frac{1}{2} [\mathbf{F}(\mathbf{x}; \theta) - \mathbf{p}]^T \mathbf{W} [\mathbf{F}(\mathbf{x}; \theta) - \mathbf{p}] \quad \text{subject to } \mathbf{R}(\theta) \leq \mathbf{0} \quad (7)$$

where \mathbf{F} , \mathbf{p} , \mathbf{x} , $\boldsymbol{\theta}$, \mathbf{W} , and \mathbf{R} represent an assumed cumulative density function vector from one of Eqs.(1)-(6), an empirical cumulative density function vector, a probability position vector, a shape parameter vector of \mathbf{F} , a weighting matrix, and a constraint vector with respect to $\boldsymbol{\theta}$. For instance, for the Gumbel distribution, the shape parameter vector consists of δ and λ in Eq.(3). Regarding the constraints \mathbf{R} , the lower constraints with respect to δ and β are imposed to ensure that the parameters lie in a feasible domain defined in Eqs.(1)-(6).

Because our concern is to accurately predict one side of tail distributions, the weighting matrix is employed to weigh the either maxima or minima values of the distribution. (Castillo 1998).

$$\mathbf{W} = \begin{cases} \text{diag}^{-1}(1 - p_m^2): \text{for maxima} \\ \text{diag}^{-1}(p_m^2): \text{for minima} \end{cases} \quad (8)$$

where p_m denotes the m^{th} component of the empirical cumulative probability vector \mathbf{p} .

Since Eq.(7) is a nonlinear function with respect to $\boldsymbol{\theta}$ and the constraints are defined to impose the lower bounds on δ and λ , a quadratic sub-problem with linear inequality constraints are employed to solve this optimization problem iteratively (Luenberger 1989).

$$\text{Min}_{\boldsymbol{\xi}} \pi_{\text{sub}} = \frac{1}{2} \boldsymbol{\xi}^T \mathbf{H}_i \boldsymbol{\xi} + \boldsymbol{\xi}^T \mathbf{g}_i \quad \text{subject to } \mathbf{A}_i \boldsymbol{\xi} - \mathbf{c}_i \leq \mathbf{0} \quad (9)$$

where $\boldsymbol{\xi}$, \mathbf{H}_i , \mathbf{g}_i , \mathbf{A}_i , and \mathbf{c}_i are an unknown solution increment vector for $\boldsymbol{\theta}$, a Hessian matrix, a gradient vector, a linear constraint matrix, and a constraint vector at i^{th} iteration, respectively. Specifically, the Hessian matrix and the gradient vector are derived as following:

$$\begin{aligned} \mathbf{H}_i &= \nabla_{\boldsymbol{\theta}} \mathbf{F}_i^T \mathbf{W} \nabla_{\boldsymbol{\theta}} \mathbf{F}_i + \nabla_{\boldsymbol{\theta}}^2 \mathbf{F}_i^T \mathbf{W} (\mathbf{F}_i - \mathbf{p}) \\ \mathbf{g}_i &= \nabla_{\boldsymbol{\theta}} \mathbf{F}_i^T \mathbf{W} [\mathbf{F}_i^T - \mathbf{p}] \end{aligned} \quad (10)$$

where \mathbf{F}_i and $\nabla_{\boldsymbol{\theta}} \mathbf{F}_i$ are the assumed cumulative density function and the first derivative of \mathbf{F} with respect to $\boldsymbol{\theta}$ at i^{th} iteration. For the simplicity of the mathematical manipulation, the subscript i is omitted hereafter.

Introducing a Lagrange multiplier vector $\boldsymbol{\mu}$, Eq.(9) can be rewritten as follows.

$$\pi_L = \frac{1}{2} \boldsymbol{\xi}^T \mathbf{H} \boldsymbol{\xi} + \boldsymbol{\xi}^T \mathbf{g} + \boldsymbol{\mu}^T (\mathbf{A} \boldsymbol{\xi} - \mathbf{c}) \quad (11)$$

Eq.(11) is rearranged into the following equation by introducing a solution vector \mathbf{q} denoting $[\boldsymbol{\xi} \ \boldsymbol{\mu}]^T$.

$$\pi_L = \frac{1}{2} \mathbf{q}^T \begin{bmatrix} \mathbf{H} & \mathbf{0} \\ \mathbf{0} & \mathbf{0} \end{bmatrix} \mathbf{q} + \mathbf{q}^T \begin{pmatrix} \mathbf{g} \\ \mathbf{A} \boldsymbol{\xi} - \mathbf{c} \end{pmatrix} \quad (12)$$

The first necessary condition of optimality is given as:

$$\nabla_{\mathbf{q}} \pi_L = \mathbf{0} \quad (13)$$

Applying Eq. (13) to Eq. (12), the first necessary condition of Eq. (9) becomes:

$$\begin{bmatrix} \mathbf{H} & \mathbf{A}^T \\ \mathbf{A} & \mathbf{0} \end{bmatrix} \mathbf{q} = \begin{pmatrix} -\mathbf{g} \\ \mathbf{c} \end{pmatrix} \quad (14)$$

Solving Eq.(14), the solution vector $\boldsymbol{\xi}$ is obtained and the solution $\boldsymbol{\theta}_{i+1}$ at the next step is updated from the current solution.

$$\boldsymbol{\theta}_{i+1} = \boldsymbol{\theta}_i + \boldsymbol{\xi} \quad (15)$$

If the solution vector $\boldsymbol{\xi}$ violates any of the constraint condition of Eq.(9), then the active set strategy (Fletcher 1971) is used to impose the inequality constraints on $\boldsymbol{\theta}$ and Eq.(9) is solved

iteratively until the all solutions lie in the feasible domain defined by the inequality conditions. The solution procedure is described in detail in the next section.

2.3 Solution Procedure for Quadratic programming with the active set strategy

The iteration described in this section is required due to inequality constraints. If no inequality constraint is triggered, there is no need for this iteration. Note that the iteration procedure in this section is the inner iteration that should be performed in each outer iteration presented in Section 2.2. Therefore, a different subscript j is used instead of I to distinguish this iteration procedure from the previous one.

1) Calculate the Hessian matrix and the gradient vector at the i^{th} iteration. Note that the Gauss-Newton Hessian is employed to approximate Hessian matrix instead of the Newton Hessian matrix because the Gauss-Newton Hessian converges better than the Newton Hessian when the optimal solution is located far from the initial guess:

$$\mathbf{H} \approx \nabla_{\theta} \mathbf{F}^T \mathbf{W} \nabla_{\theta} \mathbf{F}, \quad (16)$$

The two Hessians are almost identical when the optimal solution is near the initial guess because the second derivative term of the Newton Hessian matrix in Eq.(10) becomes negligible

2) Set the constraint matrix \mathbf{A} and the constraint vector \mathbf{c} denoting the distance between the coordinate θ_i and the boundaries of the inequality constraints. Initialize an active constraint set \mathcal{S}_0 that indicates which constraints are triggered.

3) Initialize the augmented Hessian matrix \mathbf{L} and the augmented gradient vector γ of Eq. (12).

4) Calculate the trial direction vector by solving Eq. (14):

$$\mathbf{q}_{j+1} = (\Delta \xi; \lambda_{j+1}) = -\mathbf{L}_j^{-1} \gamma_j. \quad (17)$$

5) Calculate the search step length α_i :

$$\alpha_{j+1} = \text{diag}^{-1} \{ \mathbf{A}(\xi_j + \Delta \xi) \} \mathbf{c}. \quad (18)$$

6) Find the row number k corresponding to the minimum value less than 1.0 in α_{i+1} .

$$\alpha_{j+1}^k = \min[\alpha_{j+1}, 1.0]. \quad (19)$$

where α_{j+1}^k denote the k^{th} row value of α_{j+1} . Note that if α_j^k is larger than 1.0, then the k^{th} row is set to null which means no inequality constraint is triggered.

7) Update the direction vector corresponding to the design variables:

$$\xi_{j+1} = \xi_j + \alpha_j^k \Delta \xi \quad (20)$$

8) Check out the convergence of $\Delta \xi$ and go to Step 13 if the convergence is satisfied. Otherwise processed to the next step:

$$\| \Delta \xi \| / \| \xi_{j+1} \| < \vartheta \quad (21)$$

where $\| \cdot \|$ and ϑ denote the Euclidian norm and a prescribed convergence criterion.

9) Update the active constraint set by adding the constraint index k indicating the corresponding inequality constraint is triggered. If k is null, skip this step:

$$\mathcal{S}_{j+1} \equiv \mathcal{S}_j \cup \{k\} \quad (22)$$

10) Update the Hessian matrix:

$$\mathbf{L}_{j+1} = \begin{bmatrix} \mathbf{H} & \mathbf{A}_{\mathcal{S}_{j+1}}^T \\ \mathbf{A}_{\mathcal{S}_{j+1}} & \mathbf{0} \end{bmatrix} \quad (23)$$

where $\mathbf{A}_{\mathcal{S}_{j+1}}$ denotes the active constraint matrix corresponding to the active constraint set \mathcal{S}_{j+1} .

11) Update the gradient vector:

$$\boldsymbol{\gamma}_{j+1} = \begin{pmatrix} \mathbf{g} + \mathbf{H}\boldsymbol{\xi}_{j+1} \\ \mathbf{c}_{\mathcal{S}_{j+1}} \end{pmatrix} \quad (24)$$

where $\mathbf{c}_{\mathcal{S}_{j+1}}$ denotes the active constraint vector corresponding to the active constraint set \mathcal{S}_{j+1} .

12) $j=j+1$ and go to Step 4.

13) Find out the minimum negative Lagrange multiplier and the corresponding row k . If all the Lagrange multiplier is positive then terminate the process. Otherwise,

$$\mu_{j+1}^k = \min[\boldsymbol{\mu}_{j+1}] \quad (25)$$

where μ_{j+1}^k denotes the k^{th} row value of $\boldsymbol{\mu}_{j+1}$. Note that if μ_{j+1}^k is positive, then terminate the iteration process. This means that all solutions are optimal on the hyperplane of the current active constraints.

14) Update the active constraint set by dropping the inactive constraint. If the active constraint set is empty, terminate the iteration procedure. Otherwise go to Step 10.

$$\mathcal{S}_{j+1} \equiv \mathcal{S}_j - \{k\} \quad (26)$$

3. EXAMPLES

3.1 Numerical Simulations

Simulated random signals from three different distributions are used to demonstrate the usefulness of EVS in accurately modeling the tail distributions without any prior knowledge of the parent distribution. In each example, a 99% confidence interval for the distribution is computed based on the following three methods:

1. The assumed true parent distribution.
2. A best-fit normal distribution where the sample mean and standard deviation are estimated from the sample data randomly generated from the assumed parent distribution.
3. An extreme value distribution, the parameters of which are estimated by solving the proposed nonlinear optimization for either the top or bottom fraction of the simulated random data.

Hereafter, the aforementioned three methods for the confidence interval estimation are referred to as Method 1, Method 2, and Method 3, respectively. More detailed description on these methods can be found in Sohn *et al.* 2004 regarding setting a confidence interval on the parent distribution using the above three distributions.

Three different parent distribution types are chosen to investigate the number of false-positives, or type I errors, produced by each of the three methods discussed previously. The normal, lognormal and gamma distributions are modeled using the three methods and the number of outliers is compared for a 99% confidence interval. The normal distribution provides a sanity check to make sure that the establishment of the confidence intervals based on EVS and best-fit normal distribution obtained by parameter estimation produce similar thresholds. The lognormal and the gamma distributions are both skewed and provide an opportunity to dramatically illustrate the shortcomings of the confidence interval estimation based on a normal assumption of the data.

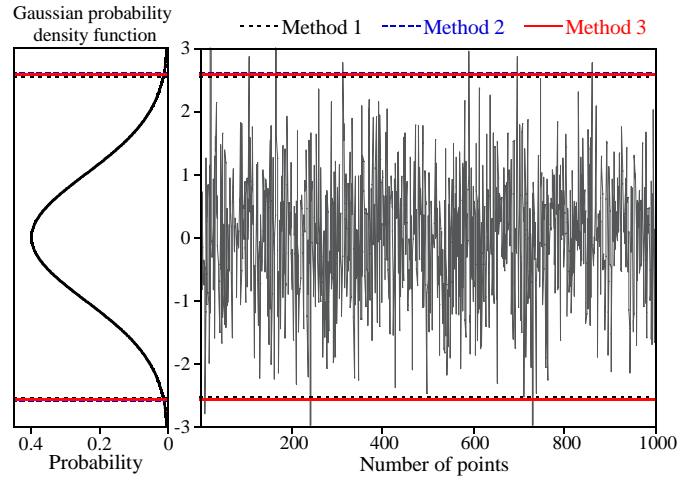


Figure 1. The exact 99% confidence interval of a normal parent distribution compared with that from extreme value distribution. This figure shows the first 1000 data points from a 10,000 data point set.

Table 2. Estimation of 99% confidence intervals for the 10,000 data points generated from a Gaussian parent distribution.

Estimation method	Upper confidence Limit	Lower confidence Limit	# of outliers out of 10,000 samples. ($\alpha = 0.01$)
Method 1 (Exact)	2.548	-2.548	100
Method 2 (Normal)	2.602	-2.581	96
Method 3 (Gumbel)	2.576	-2.561	100

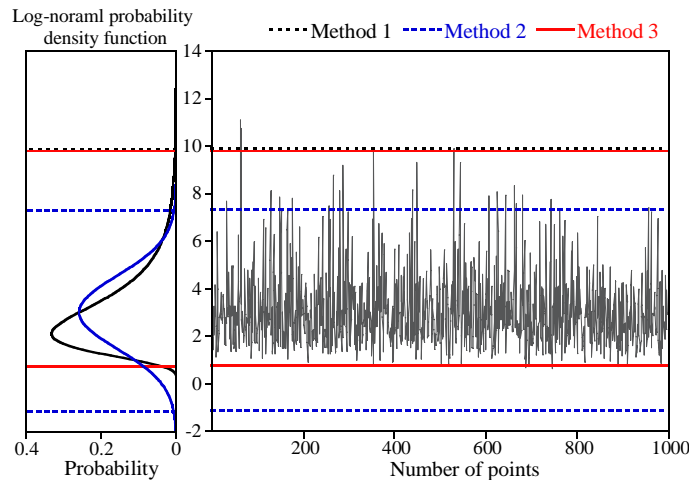


Figure 2. The exact 99% confidence interval of a lognormal parent distribution with those computed from either extreme value distribution or the normality assumption.

Table 3. Estimation of 99% confidence intervals for the 10,000 data points generated from a lognormal parent distribution.

Estimation method	Upper confidence Limit	Lower confidence Limit	# of outliers out of 10,000 samples. ($\alpha = 0.01$)
Method 1 (Exact)	9.854	0.750	100
Method 2 (Normal)	7.278	-1.160	241
Method 3	9.771	0.7357	109

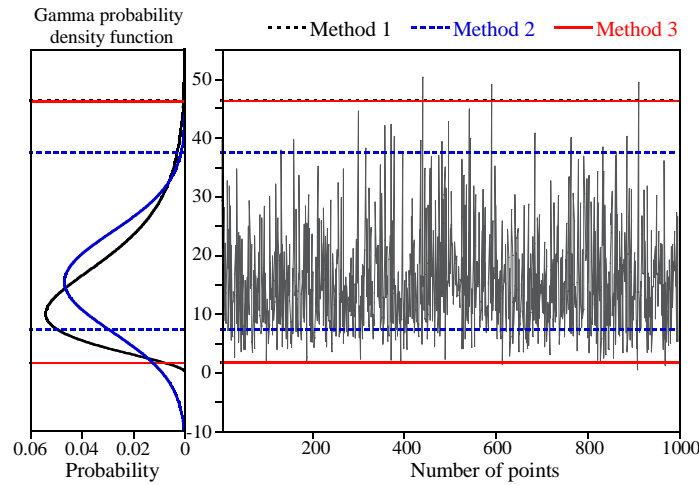


Figure 3. The exact 99% confidence interval of a gamma parent distribution with those computed from either extreme value distribution or the normality assumption.

Table 4. Estimation of 99% confidence intervals for the 10,000 data points generated from a gamma parent distribution

Estimation method	Upper confidence Limit	Lower confidence Limit	# of outliers out of 10,000 samples. ($\alpha = 0.01$)
Method 1 (Exact)	46.369	1.689	100
Method 2 (Normal)	37.56	-7.257	223
Method 3 (Gumbel)	46.240	1.684	105

3.2 Parameter Estimation of Extreme Value Distribution using Real Sample Data

The proposed parameter estimation technique is applied to estimate the statistical distributions of real extreme value data such as Maximum wind velocity data, epicenter data, and fatigue data published in Castillo 1998.

Table 5 shows the residuals of the converged error function defined in Eq. 7. For each data set, the smallest residuals are denoted in bold and the best-fit distribution corresponding to the smallest residuals is listed in the last column of Table 1. To validate the proposed selection criterion for extreme value distributions, the extreme value distributions selected by other selection methods are presented in Table 6. It is concluded that the extreme distributions selected by the proposed method agree with those estimated by other methods (Castillo 1998). In addition, it should be noted that the proposed method is superior to the other methods in a sense that the final residuals using the proposed method are smaller than those from the other methods

Figure 4 shows the estimated cumulative density functions and empirical cumulative density functions based on the best-fit extreme value distribution for each data set. Note that data points with the smallest values are best fitted of all data points especially when Epicenter data are used. This is because the weighting matrix of Eq.(8) plays an important role in weighing either maxima or minima values of the distribution. Finally, regarding the stability of the nonlinear optimization used for parameter estimation, all solutions are obtained successfully in a few iterations.

Table 5. Selecting the best-fit EV distribution based on the converged error function

Sample Data	Residuals of Converged Error Function			Best-fit EV dist.
	Weibull	Gumbel	Frechet	
Wind (+)*	1.1103	1.0761	0.19692	Frechet
Epicenter (-)	0.74287	6.7358	6.9779	Weibull
Fatigue (-)	0.17664	2.1031	2.1873	Weibull
Wave (+)	0.085799	0.084634	0.095251	Gumbel

* (+) and (-) denote maxima and minima of the sample data.

Table 6. Comparison with other methods to decide domain of attractions

	Probability paper	Picklands III	Curvature method	This study
Wind (+)	Gumbel or Frechet	Gumbel	Frechet	Frechet
Epicenter (-)	Weibull	Weibull	Weibull	Weibull
Fatigue (-)	Weibull	Weibull	Weibull	Weibull
Wave (+)	Gumbel	Gumbel	Gumbel	Gumbel

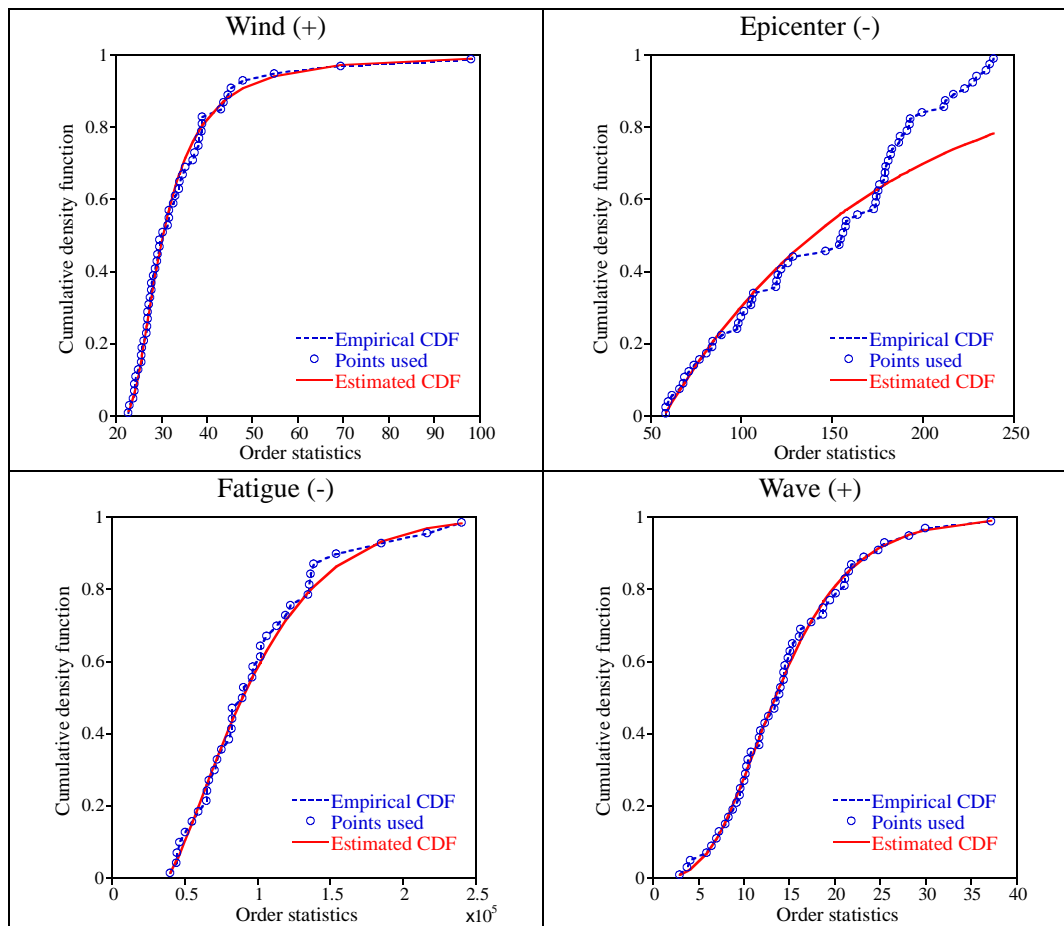


Figure 4. Estimated cumulative probability (red line) using each best-fit EV distribution and empirical

cumulative probability (blue line) using each sample data.

3.3 Application to Damage Detection of a Composite Plates

The overall test configuration of this study is shown in Figure 5 (a). The test setup consists of a composite plate with a surface mounted sensor layer, a personal computer with a built-in data acquisition system, and an external signal amplifier. The dimension of the composite plates is 60.96 cm x 60.96 cm x 0.6350 cm (24 in x 24 in x 1/4 in). A total of 16 PZT patches are used as both sensors and actuators to form an “active” local sensing system. Because the PZTs produce an electrical charge when deformed, the PZT patches can be used as dynamic strain gauges. Conversely, the same PZT patches can also be used as actuators, because elastic waves are produced when an electrical field is applied to the patches. In this study, one PZT patch is designated as an actuator, exerting a predefined waveform into the structure. Then, the adjacent PZTs become strain sensors and measure the response signals. This actuator-sensor sensing scheme is graphically shown in Figure 5 (b). This process of the Lamb wave propagation is repeated for different combinations of actuator-sensor pairs. A total of 60 different path combinations are investigated in this study. Actual delamination is seeded to the composite plate by shooting a steel projectile into the composite plate. The data collection using the active sensing system was performed before and after the impact test.

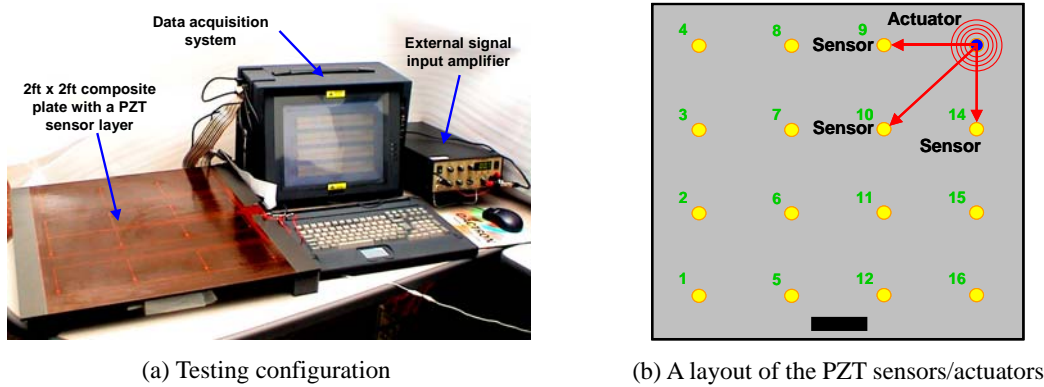


Figure 5: An active sensing system for detecting delamination on a composite plate

In this study, a damage detection method is developed based on time reversal acoustics. According to the time reversal concept, an input signal can be reconstructed at an excitation point (point A) if an output signal recorded at another point (point B) is reemitted to the original source point (point A) after being reversed in a time domain as shown in Figure 6. This process is referred to as the time reversibility of waves. This time reversibility is based on the spatial reciprocity and time-reversal invariance of linear wave equations (Fink and Prada 2001). However, it should be noted that time reversal acoustic is originally developed for propagation of body waves in an infinite solid media. Additional issues such as the frequency dependency of time reversal operator and signal reflection due to limited boundary conditions should be addressed to successfully achieve the time reversibility for Lamb waves. By developing a unique combination of a narrowband excitation signal and wavelet-based signal processing techniques, the authors demonstrated previously that the original input waveform could be successfully reconstructed in a composite plate through the enhanced time reversal method (Park et al. 2004).

This paper takes advantage of this enhanced time reversal method to identify defects in composite plates: Damage causes wave distortions due to wave scattering during the time reversal process and it breaks down the linear reciprocity of wave propagation. Therefore, a damage index is defined as a function of the reconstructed signal's deviation from the original input waveform:

$$DI = 1 - \sqrt{\frac{\left\{ \int_{t_0}^{t_1} I(t)V(t) dt \right\}^2}{\left\{ \int_{t_0}^{t_1} I(t)^2 dt \int_{t_0}^{t_1} V(t)^2 dt \right\}}} \quad (27)$$

where the $I(t)$ and $V(t)$ denote the known input and reconstructed signals. t_0 and t_1 represent the starting and ending time points of the baseline signal's first A_0 mode. The value of DI becomes zero when the time reversibility of Lamb waves is preserved. Note that the root square term in Eq. (27) becomes 1.0 if and only if $V(t) = \beta I(t)$ for all t where $t_0 \leq t \leq t_1$ and β is a nonzero constant. Therefore, a simple linear attenuation of a signal will not alter the damage index value. If the reconstructed signal deviates from the input signal, the damage index value increases and approaches 1.0, indicating the existence of damage along the direct wave path. It should be noted that the proposed damage detection method leaves out unnecessary dependency on past baseline signals by instantly comparing the known input signal to the reconstructed input signal. By eliminating the need for the baseline signals, the proposed damage detection is immune to potential operational and environmental variations throughout the life span of a structure.

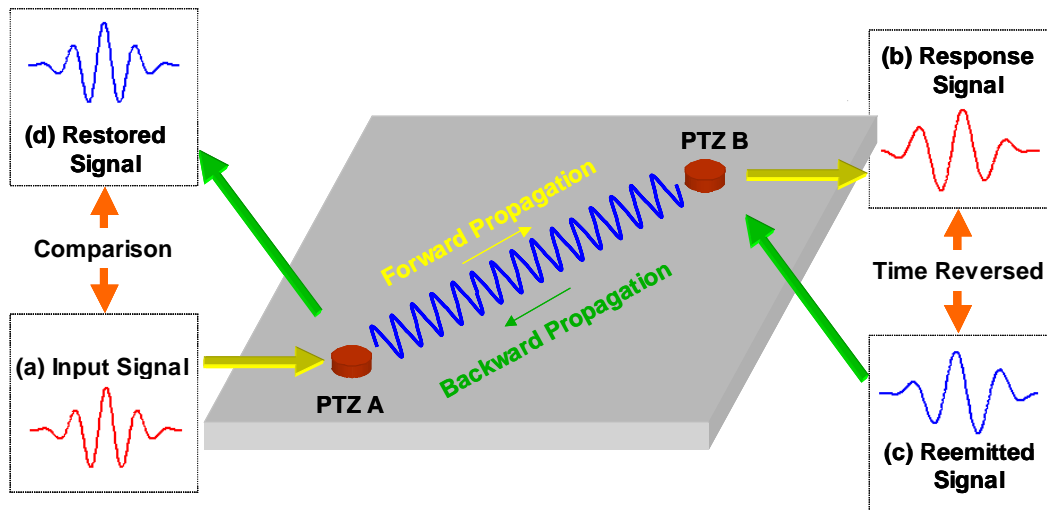


Figure 6: A schematic concept of damage identification in a composite plate through time reversal processes

The next step is to compute a threshold value. Once the damage index value exceeds a pre-specified threshold value, the corresponding actuator-sensor path is defined as damaged. First, the damage index values were computed for all 66 paths when there was no damage on the plate. Then, one of the extreme value distributions was fitted to the damage index values as shown in Figure 7 (a). In this example, the Weibull distribution turned out to best describe the damage index values. Once the parameters of the Weibull distribution was estimated by the presented quadratic programming, a threshold value corresponding to a 99.9% confidence level was established in Figure 7 (b).

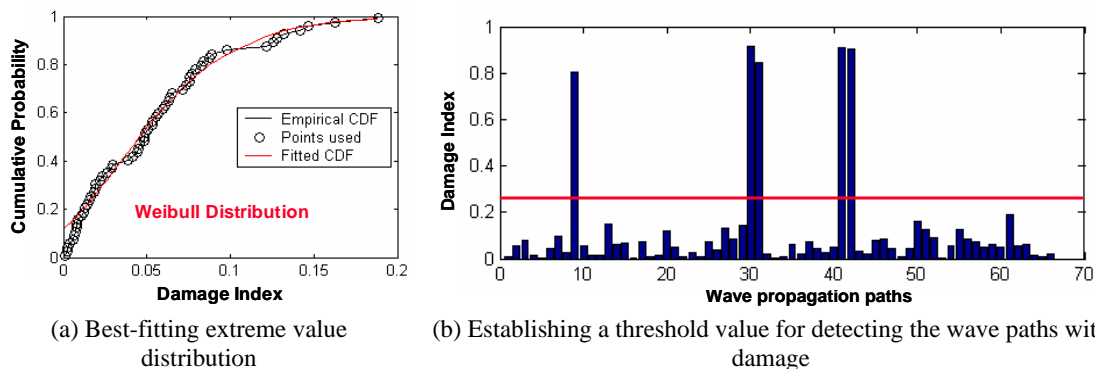


Figure 7: Threshold establishment using Extreme Value Statistics

Figure 8 (a) shows the actual impact location. The identification of the damaged paths shown in Figure 8 (b) is based on the results shown in Figure 7 (b). The final goal is to pinpoint the location of

delamination and to estimate its size based on the damaged paths identified in Figure 8 (b). To identify the location and area of the delamination, a damage localization algorithm is also developed in Sohn et al. 2004. The delamination location and size estimated by the active sensing system was presented in Figure 8 (c), and the estimate from the proposed damage identification matched well with the ultrasonic scan results.

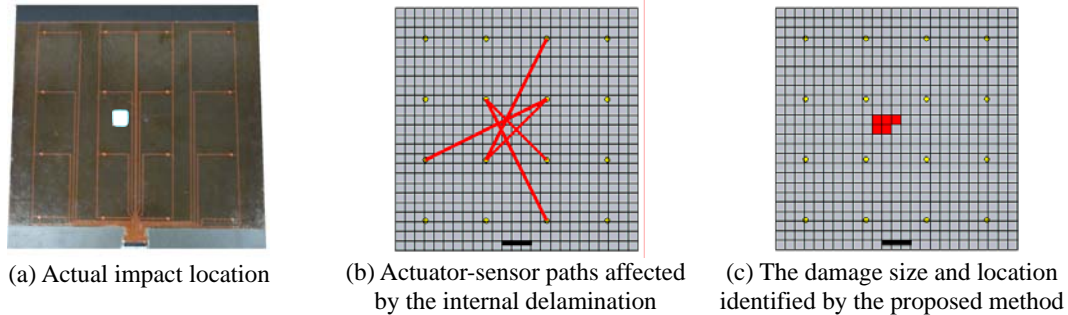


Figure 8: Detection of different sizes of damage using the wavelet-based approach

4. SUMMARY

Data that lie in the tails of distributions have traditionally been modeled based on a Gaussian distribution. This inherent assumption of many statistical processes can be dangerous for applications such as damage detection, which deal mostly with those extreme data points that may not be accurately modeled by the Gaussian assumption. Extreme value statistics (EVS) focuses on modeling those extreme points without knowing their parent distributions. Modeling the tails simplifies the decision-making (establishment of decision boundaries) to some extent because the extreme values follow one of three EV distributions. These extreme points conform to one of three types of distributions: Gumbel, Weibull, or Frechet. In this paper, the damage detection is reworked to take advantage of these extreme value distributions.

A quadratic programming technique for solving nonlinear optimization problems is adopted to automatically estimate the parameters of the extreme value distributions. In particular, no specific type of the distribution for each sample data needed to be known *a priori*. The first numerical examples demonstrated the effectiveness of EVS when applied to a simple novelty analysis. Thresholds obtained from the actual distribution, the best-fit normal distribution and the extreme value distributions were compared. In all of the examined cases, EVS produced results that only slightly deviated from those of the true distributions. In the second example, it was shown that the best-fit extreme distribution can be determined *a posteriori* by applying the presented parameter estimation technique to real sample data. Finally, EVS is incorporated into a delamination detection study where delamination in a composite plate was successfully detected by using PZT materials for sensing and actuation.

REFERENCES

- Worden, K., Manson, G. and Fieller, N.J., "Damage Detection Using Outlier Analysis", *Journal of Sound and Vibration*, vol.229, 2000a, pp.647-667.
- Roberts, S., *Novelty Detection Using Extreme Value Statistics*, IEE Proceedings in Vision, Image and Signal Processing, vol.146, pp.124-129.
- Roberts, S., *Extreme Value Statistics for Novelty Detection in Biomedical Signal Processing*, IEE Proceedings in Science, Technology and Measurement, vol.147, 2000, pp.363-367.
- Worden, K., Pierce, S.G, Manson, G, Philip, W.R., Staszewski, W.J. and Culshaw, B., "Detection of

Defects in Composite Plates using Lamb Waves and Novelty Detection,” *International Journal of System Science*, vol.31, 2000b, pp.1397-1409.

Kramer, S.L., *Geotechnical Earthquake Engineering*, Prentice Hall, Upper Saddle River, NJ, 1996.

Benjamin, J.R. and Cornell, C.A., *Probability, Statistics and Decision for Civil Engineers*, McGraw-Hill, Inc. New York, NY. 1970.

Fisher, R.A. and Tippett, L.H.C., “Limiting Forms of the Frequency Distributions of the Largest or Smallest Members of a Sample,” *Proceedings of the Cambridge Philosophical Society*, vol.24, 1928, pp.180-190.

Castillo, E., *Extreme Value Theory in Engineering*, Academic Press Series in Statistical Modeling and Decision Science, San Diego, CA, 1998.

Luenberger, D.G., "Linear and Nonlinear Programming, Second Edition", Kluwer Academic Publishers, 1989.

Fletcher, R., “A general quadratic programming algorithm,” *Journal of Institute of Mathematics and its Applications*. 7 pp. 76-91, 1971

Sohn, H., Allen, D.W., Worden, K., and Farrar, C.R., “Structural damage classification using extreme value statistics”, *ASME Journal of Dynamics Systems, Measurements, and Control*, 2004, in press.

Wirsching, H., Paez, T. L. and Ortiz, K., *Random Vibrations Theory and Practice*, John Wiley, New York, NY, 1995.

Fink, M. and Prada, C. (2001). “Acoustic time-reversal mirrors.” *Inverse Problems*, 17, R1-R38.

Park, H. W., Sohn, H., Law, K. H., and Farrar, C. R. (2004). “Time reversal active sensing for health monitoring of a composite plate.” *submitted for publication of Journal of Sound and Vibration*.

Sohn, H., Park, G., Wait, J. R., Limback, N. P., and Farrar, C. R. (2004). “Wavelet-based active sensing for delamination detection in composite structures.” *Smart Materials and Structures*, 13(1), 153-160.